Iraqi Journal of Physics, 2026
https://doi.org/10.30723/ijp.v24i2.1546

Vol.24, No.2, PP.12-20
P-ISSN: 2070-4003
E-ISSN: 2664-5548

Thermally Tuned Distributed Bragg Reflector Optical Biosensor with Blood Cavity for Malaria Detection: Resonance Tracking, Thermal Sensitivity, and Field Localization Analysis

Sadiq Abdullah Muhamad AL-Jabhah[1*] and Fahem Yehya Ahmed Bajash[1]
Department of Physics, Faculty of Education and Science, Albaydha University, Yemen
*Corresponding author: sadiqaljabha@baydaauniv.net

Abstract

This work presents a numerical study of a multilayer optical biosensor based on distributed Bragg reflectors (DBRs) with a blood-filled cavity. The Transfer Matrix Method (TMM) was employed and simulated in MATLAB to analyze the resonant behavior over the wavelength range 780-810 nm. The analysis also considered the effects of temperature variation from 15 to 40 °C and changes in the silicon layer thickness from 20 to 200 nm. The results revealed a blue shift in the resonant wavelengths of the defect mode due to temperature variation, leading to a negative thermal sensitivity whose magnitude depends nonlinearly on the silicon layer thickness. In addition, electric field intensity distributions at resonance revealed stronger localization of the mode within the cavity for intermediate silicon layer thicknesses. This increases the interaction between light and matter and broadens the spectral shift range induced by temperature changes. Conversely, thick silicon layers redistribute optical energy in the Bragg mirrors, compensating for thermal drift with partial compensation occurring due to redistribution. The results show that the performance of resonance confinement and temperature response can be significantly enhanced through geometric tuning, demonstrating the potential application of this design as an optical biosensor for malaria-related blood diagnostics without requiring labels.

Article Info.

Keywords:
Bragg, Biosensor, Thermo-Optic, Malaria, Distributed Bragg Reflectors.

Article history:
Received: Jan. 27, 2026
Revised: Feb. 22, 2026
Accepted:Mar.13, 2026
Published:Jun. 01,2026

1. Introduction

Multilayer photonic structures for optical biosensing are now at the forefront of modern biomedical diagnostics due to their high spectral selectivity, compactness, and compatibility with label-free interrogation schemes [1, 2]. One-dimensional photonic crystals and Distributed Bragg Reflector (DBR) cavities are particularly appealing, as they support narrow defect resonances with photonic band gaps, allowing for high-resolution resonance tracking in response to perturbations of the cavity refractive index or temperature [3-5]. Recent investigations have demonstrated that DBR-type resonators can achieve extremely high-quality factors and refractive-index sensitivities when their geometrical parameters are carefully optimized [5,6]. Such architectures have, therefore, been extensively proposed for biochemical and hematological sensing, including optical interrogation of blood properties [7-9].

In recent years, increasing attention has been directed toward the detection of malaria using photonic sensors based on optical cavities. This approach relies on changes in infected red blood cells, which affect both the refractive index and optical scattering properties. These variations lead to shifts in resonance wavelengths that can be measured using such sensors [10–12]. In addition, theoretical studies have demonstrated the potential of defect-based photonic sensors for diagnosing malaria at its different stages and for distinguishing between various blood components. This contributes to the development of advanced biosensing devices and improves their performance [13, 14]. Nevertheless, several challenges still affect the performance of photonic sensors, such as thermal drift. Temperature directly influences the refractive index within the cavity and the Bragg mirrors, changing the optical path length within

the sensor and obscuring its weak signals. Therefore, efficient system design is essential to mitigate these challenges [15,16].

Accordingly, recent literature and studies have focused on identifying and controlling the thermo-optical response in cavity-based medical biosensors [17, 18]. Since significant technological advances have already been achieved in this field, little research has yet been presented on the aforementioned influence of Bragg mirrors and the silicon layer thickness with regard to resonance confinement versus localization of electromagnetic field distribution, as well as thermal sensitivity. Upon reviewing the existing literature, it was found that some studies have mainly addressed various types of sensing mechanisms derived from variations in their refractive index and the most commonly discussed temperature suction forces, but as a separate phenomenon without establishing a direct link between varying geometrical dimensions and redirected resonant modes within the cavity [19, 20].

As red blood cells are infected by malaria, their chemical composition and structural properties change, which changes their optical properties. The refractive index of healthy blood has previously been reported to range from 1.38 to 1.40 [9–11]. Rather than simulating conditions of malaria infection, this study targets the optimization of thermo-optical parameters for a distributed Bragg reflector cavity biosensor platform. By improving resonance confinement and thermal sensitivity, photonic structures are capable of identifying even maximal variations in refractive index related to pathological changes due to malaria infection or other hematological conditions. [10–13].

In this work, a comprehensive numerical investigation of a DBR-blood-DBR multilayer optical biosensor using the transfer matrix method is presented. The temperature-dependent resonance behavior is analyzed over the physiological range, and the extracted thermal sensitivity is correlated with the internal electric-field distribution to identify silicon thickness regimes that maximize cavity confinement and sensing performance, thereby providing design guidelines for thermally tunable biosensors targeting malaria-related blood diagnostics.

2. Numerical Model and Computational Methods

The optical response of the proposed distributed Bragg reflector multilayer optical biosensor was analyzed using the Transfer Matrix Method (TMM), which enables accurate computation of reflectance spectra, resonance wavelengths, and internal electromagnetic field distributions in stratified media by enforcing electromagnetic boundary conditions at each interface [3, 4, 19]. The structure of the distributed Bragg reflector multilayer optical biosensor consists of two symmetric distributed Bragg reflectors enclosing a blood-filled cavity of 7 μm thickness. Each mirror is composed of six alternating layers of silicon (Si) and silicon dioxide (SiO_2), a combination widely used in near-infrared photonic devices due to its high refractive-index contrast and technological compatibility [15, 18].

In these studies, the number of Bragg periods, previously described, was determined in a way that ensures the formation of a sufficiently wide stop band, as reported in several previous studies [5, 6]. A schematic diagram of the proposed multilayer biosensor structure is presented in Fig. 1, showing alternating Si/SiO_2 Bragg mirrors and the central blood cavity. This configuration enables the formation of a photonic stopband and supports a localized defect resonance inside the cavity [5,6].

The silicon layer thickness was varied from 20 to 200 nm in 20 nm increments, while the SiO_2 thickness was fixed at 300 nm. Similar thickness-tuning approaches have been reported to significantly influence defect-mode confinement and sensitivity in photonic biosensors [5-7]. Reflectance spectra were calculated at normal incidence over 780-810 nm, a spectral window suitable for blood analysis owing to relatively low absorption [8, 9]. The resonance wavelength was identified as the reflectance minimum corresponding to the cavity mode [10,11].

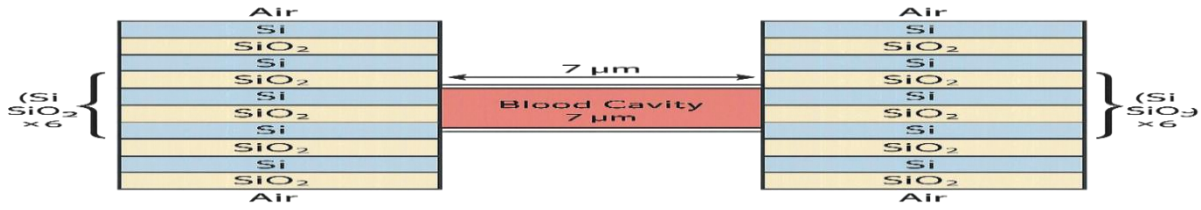

Figure 1: A schematic diagram of the distributed Bragg reflector multilayer optical biosensor with a blood-filled cavity showing alternating Si/SiO_2 layers and the central defect region.

Temperature-dependent refractive indices of all layers were incorporated using reported thermo-optic coefficients [15-17]. The temperature was changed from 15 to 40 °C. Thermal sensitivity was extracted from the slope of the resonance wavelength versus temperature. The TMM describes the propagation of electromagnetic waves through multilayer structures by relating the electric and magnetic fields at the input and output interfaces. For each layer, the characteristic matrix is expressed in Eq. (1):

$$M\_i = \begin{matrix} \cos(\delta_i) & \left(\frac{i}{\eta\_i}\right)\sin(\delta_i) \\ i\,\eta_i\sin(\delta_i) & \cos(\delta_i) \end{matrix} \quad (\mathbf{1})$$

where $\delta_i = (2\pi n_i d_i)/\lambda$ represents the phase thickness, η_i is the refractive index, d_i is the layer thickness, and λ is the wavelength of incident light.

The overall transfer matrix of the multilayer structure is obtained by multiplying the individual matrices, as in Eq. (2):

$$M = \prod_{i=1}^{n} M_i \quad (\mathbf{2})$$

The reflectance of the multilayer system is calculated using the matrix elements, as in Eq. (3):

$$R = \left|\frac{M21}{M11}\right|^2 \quad (\mathbf{3})$$

Resonance occurs when constructive interference inside the cavity leads to strong electromagnetic field localization and a corresponding minimum reflectance. This resonant state exhibits a precise spectral pathway for biological and biomedical applications [19, 20]. The values used in the present study, such as material parameters, refractive indices, and thermo-optic response coefficients, were adopted from previously published and well-established studies [8, 15-17].

The present work employed numerical analysis as a simulation approach rather than an experimental study. In addition, the study relied on the optical properties of blood reported in previously validated research [9-11]. To support this framework, a numerical simulation was performed under the same optical and physiological conditions relevant to malaria diagnosis.

3. Results and Discussion

3.1. Thermal Sensitivity and Silicon Thickness

Fig. 2 illustrates the thermal sensitivity resulting from temperature-dependent resonance as a function of the silicon layer thickness. The relationship is shown to be non-monotonic. The thermal sensitivity increases until it reaches approximately 80 nm, after which it decreases

with further increases in the silicon layer thickness. Accordingly, the maximum optimal thermal sensitivity occurs at a silicon thickness of 80 nm. This behavior can be attributed to the improved optical confinement and the strong enhancement of the electromagnetic field inside the blood cavity, which leads to a greater resonance wavelength shift induced by temperature variations.

Furthermore, Fig. 2 also indicates a secondary increase in sensitivity at larger silicon thicknesses. This phenomenon is associated with partial resonance coupling and redistribution of the electromagnetic field within the cavity, although this enhancement remains weaker than the primary peak sensitivity. From the above observations, it can be concluded that moderate silicon thicknesses around 80 nm provide the optimal optical confinement. When the thickness increases further, the thermal sensitivity decreases despite the improved mirror reflectivity.

This behavior is mainly attributed to the redistribution of the optical field within the Bragg mirrors, along with partial thermal compensation effects.

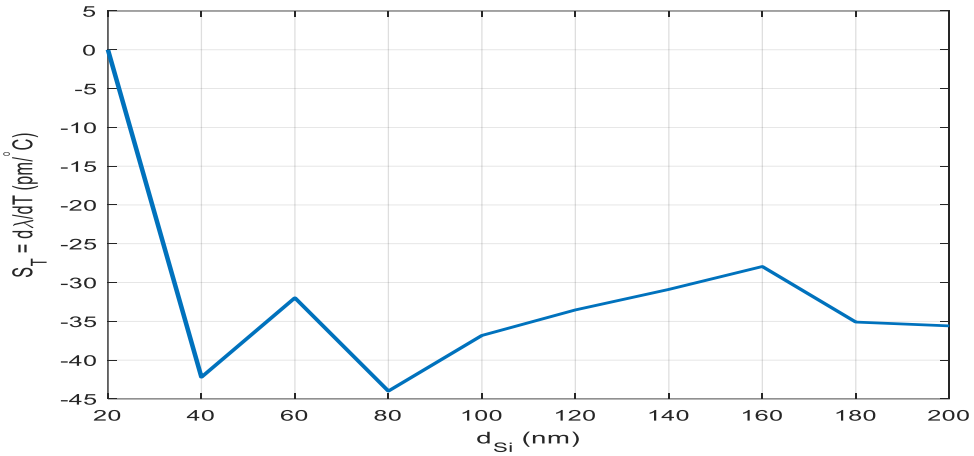

Figure 2: Thermal sensitivity as a function of silicon layer thickness.

3.2. Temperature-Dependent Resonance Shift

Fig. 3 illustrates the relationship between the resonance wavelength and temperature for different silicon layer thicknesses; all configurations show a blue shift in the resonance wavelength as the temperature increases from 15 to 40 °C. The relationship appears to be approximately linear within the studied range. This behavior can be attributed to the thermo-optic changes in the cavity medium and in the layers surrounding the Bragg mirrors within the sensor structure.

3.3. Reflectance Spectrum and Defect-Mode Formation

Fig. 4 shows the reflection spectrum in the presence of a defect mode within the cavity; the sharp spectral feature indicates the formation of a defect mode supported by the DBR mirrors. This behavior demonstrates the suitability of the structure for high-resolution spectral analysis.

The narrow and pronounced dip observed in Fig. 4 indicates a high-quality factor (Q-factor), which reflects strong optical confinement inside the cavity. This characteristic enhances spectral precision and improves the biosensor's ability to detect small variations in refractive index and temperature, indicating its suitability for high-sensitivity sensing applications.

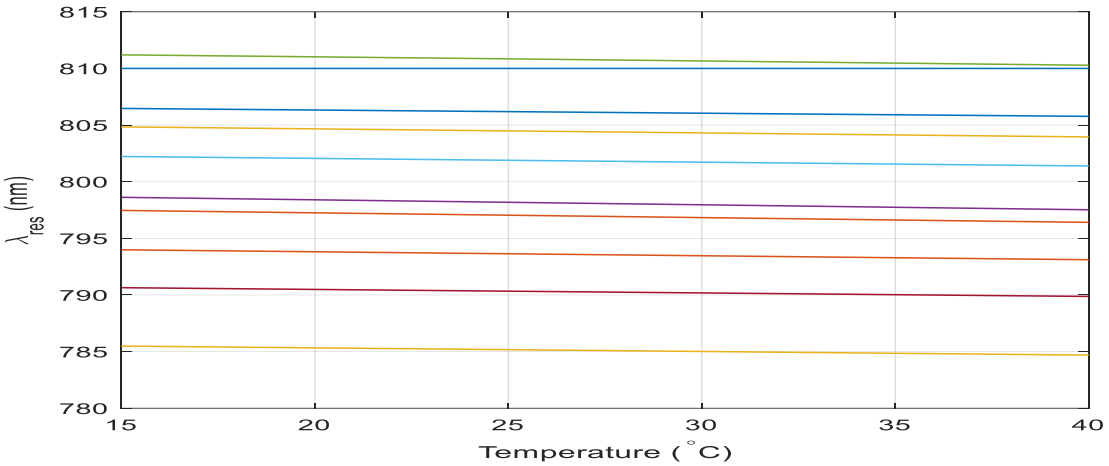

Figure 3: Variation of the resonance wavelength (λ(res)) as a function of temperature for silicon layer thicknesses ranging from 20 nm to 200 nm with a step of 20 nm. Each curve represents a different silicon thickness.

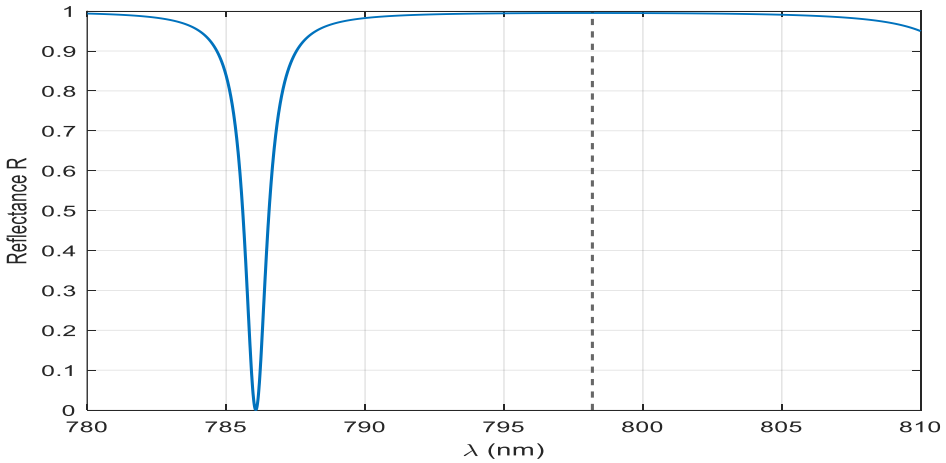

Figure 4: Reflectance spectrum showing the cavity resonance within the Bragg stopband.

3.4. Electric-Field Localization Analysis

To understand the physical relationship of silicon layer thickness with sensor performance, three representative thicknesses, small (20 nm), medium (80 nm), and large (180 nm), were selected for electric field distribution analysis. These thicknesses were selected based on the trend in thermal sensitivity depicted in Fig. 2. As shown above, the 20 nm thickness provides weak optical confinement, whereas the 80 nm thickness provides good confinement and maximum thermal sensitivity. In comparison, the 180 nm thickness shows a decrease in sensitivity due to the rearrangement of the electromagnetic field.

This choice then allows us to establish a direct connection between electromagnetic field localization and the thermal behavior, as reported in previous works [8,14]. The 3D electric field intensity maps at resonance are shown in Figs. 5–7 for different silicon layer thicknesses.

At a thickness of 20 nm (Fig. 5), the confinement is weak, and the electric field penetrates deeply into the DBR stacks. Such a method minimizes the interaction with the blood-filled cavity and therefore decreases thermal sensitivity. At 80 nm thickness (Fig. 6), the electric field is strongly focused in the interaction with the blood cavity. This favors cavity light–matter interaction and, subsequently, leads to the highest thermal sensitivity seen in Fig. 2. In Fig. 7, at a thickness of 180 nm, however, a significant part of the optical energy gets

trapped between the DBR mirrors. This leads to a partial thermal compensation and a decrease in the resonance wavelength variation. By analyzing optical phase matching and resonant confinement, the evolution of the electric field distribution with thicker silicon can be studied.

At small thicknesses, there are not enough layers to properly confine the cavity; thus, the electromagnetic field can penetrate deeply into DBR mirrors. The spacing of the resonators can also lead to constructive interference, resulting in an enhancement of the electric field localized in the blood cavity at intermediate thicknesses (80 nm). This enhances light–matter interactions and increases thermal sensitivity.

For larger thicknesses of 180 nm, the increase in thickness changes the resonance conditions and partially redistributes the electromagnetic field into the DBR mirrors. Consequently, the effective optical confinement factor within the cavity is reduced, negatively affecting sensing performance. Based on the above analysis, it can be inferred that a direct correlation exists among silicon thickness, electric field distribution, and thermal sensitivity response, whereby an optimal silicon thin film affords the maximum resonant confinement, thereby yielding the highest sensor sensitivity.

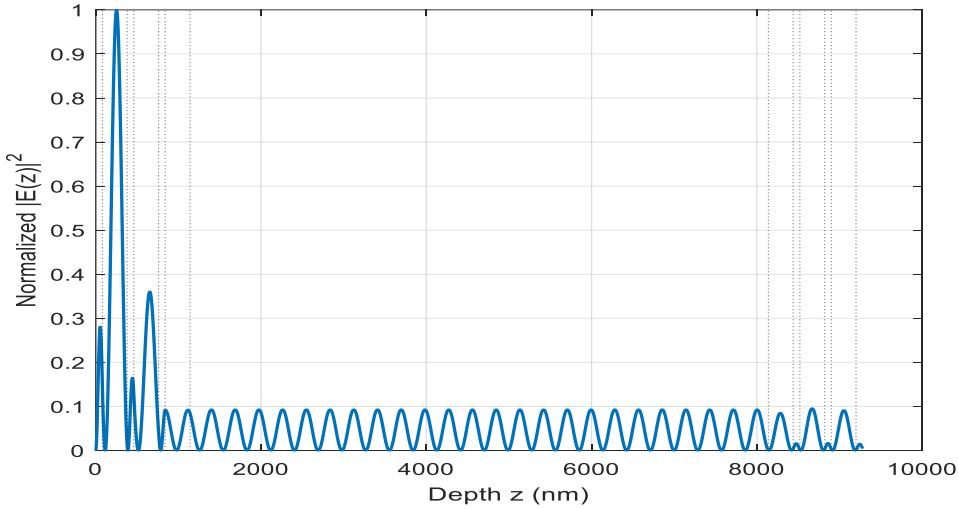

Figure 5: Electric field intensity distribution at resonance for Si layer thickness of 20 nm.

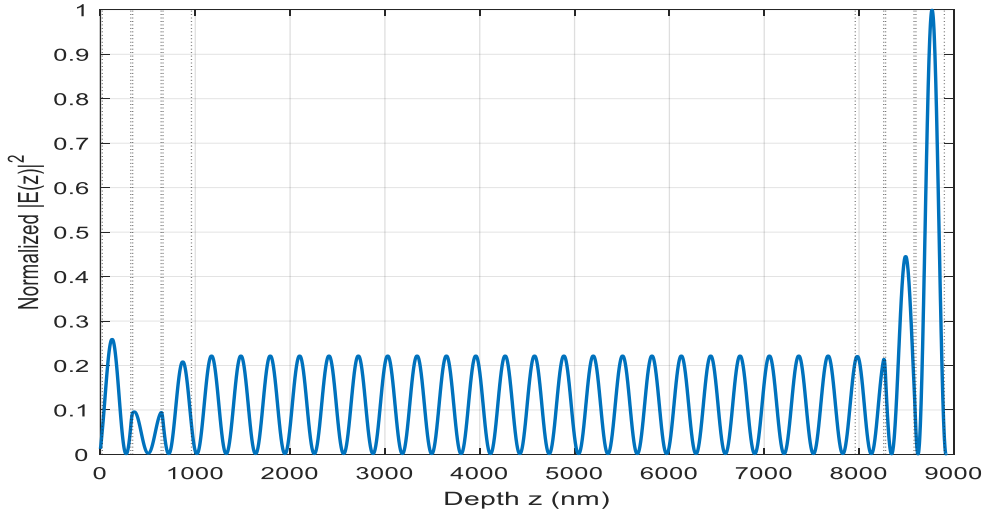

Figure 6: Electric field intensity distribution at resonance for silicon layer thickness of 80 nm.

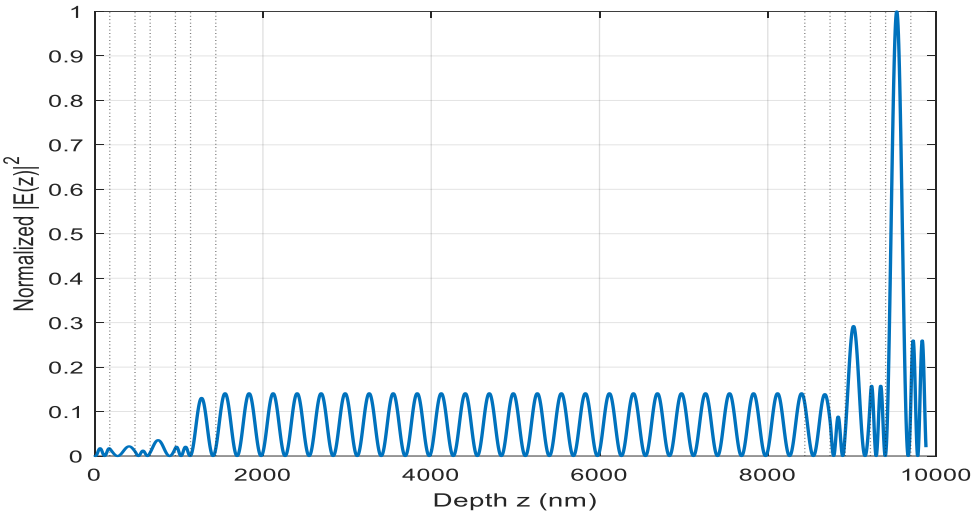

Figure 7: Electric field intensity distribution at resonance for silicon layer thickness of 180 nm.

3.5. Implications for Biosensing Applications

The results demonstrate that thermal sensitivity in the proposed DBR–blood–DBR multilayer biosensor is strongly influenced by silicon layer thickness and the resulting electric-field localization within the cavity. By selecting an optimal silicon thickness, enhanced optical confinement within the blood layer can be achieved, improving light–matter interactions and temperature-dependent resonance response. These findings highlight the importance of geometrical tuning in optimizing sensing performance for the specific multilayer structure investigated in this study.

4. Conclusions

In this study, a symmetric DBR–blood–DBR multilayer optical biosensor was numerically investigated with emphasis on temperature-dependent resonance behavior, Si layer thickness optimization, and electromagnetic field localization. Using the transfer matrix method, the influence of geometrical tuning on resonance confinement and thermo-optic response was systematically analyzed within the near-infrared spectral range. The results revealed a consistent blue shift in the resonance wavelength with increasing temperature within the investigated region, enabling accurate analysis of thermal sensitivity. Moreover, the results showed that thermal sensitivity strongly depends on the silicon layer thickness. The maximum response was achieved at a silicon layer thickness of 80 nm with the highest obtained thermal sensitivity value (-43.99 pm/°C). This suggests a strong thermo-optic response in the blood cavity due to the strong confinement of the EM field inside it. In addition, the electric field simulation showed that this optimal thickness is where the field is most localized, which greatly improves light-blood interactions and lessens thermal compensation due to Bragg mirrors. These findings emphasize the importance of structural design optimization to enhance sensing performance, as well as demonstrating the potential of the designed DBR–blood–DBR structure for accurate retrieval of temperature and refractive index. The sensitivity attained is considerable in the context of biosensing applications; thus, the suggested structure could be the key to constructing integrated optical biosensors, which might find applications in clinical malaria detection and related biomedical usages.

Conflict of Interest

The authors declare that they have no conflict of interest.

References

1. L. Liu, J. Tibbs, N. Li, A. Bacon, S. Shepherd, H. Lee, N. Chauhan, U. Demirci, X. Wang, B. Cunningham, A photonic resonator interferometric scattering microscope for label-free detection of nanometer-scale objects with digital precision in point-of-use environments, *Biosens. Bioelectron,* **228**, 115197 (2023). https://doi.org/10.1016/j.bios.2023.115197.
2. J. Homola, Surface Plasmon Resonance Sensors for Detection of Chemical and Biological Species, *Chem. Rev*. **108**(2), 462 (2008). https://doi.org/10.1021/cr068107d.
3. P. Yeh, Optical Waves in Layered Media (Wiley, New York, 1988).
4. J. D. Joannopoulos, S. G. Johnson, J. N. Winn, and R. D. Meade, Photonic Crystals: Molding the Flow of Light, second edition (*Princeton Univ. Press, Princeton*, 2008).
5. M. Sovizi and M. Aliannezhadi, Highly sensitive asymmetric and symmetric cancer sensors with ultra-high-quality factor and resolution power, *Sci. Rep*. **13**, 12251 (2023). https://doi.org/10.1038/s41598-023-39422-w.
6. J. Zaghdoudi, I. H. Giden, and M. Kanzari, *Physica B: Condensed Matter*, Next-generation 1D photonic crystal sensor: Revolutionizing fat concentration measurement in commercial milk, **714**, 417428 (2025). https://doi.org/10.1016/j.physb.2025.417428.
7. D. M. Nasr, S. I. Mostafa, and M. A. El Naggar, Annular photonic crystal biosensor for blood components and blood infections. *Eur. Phys. J. D* **79**, 39 (2025). https://doi.org/10.1140/epjd/s10053-025-00970-7.
8. N. Bilgili and A. Çetin, Design and analysis of a highly sensitive one-dimensional photonic crystal biosensor for the detection of diabetes in human tears, *Mol. Cryst. Liq*. Cryst. **770**(2), (2026). https://doi.org/10.1080/15421406.2025.2598658.
9. A. M. Mohamed, W. Sabra, M. Mobarak, A. S. Shalaby, and Arafa H. Aly, Design of a 1D PhC biosensor with enhanced sensitivity based on useful features provided for the detection of waterborne bacteria, Opt. Quantum Electron. 56, 433 (2024), https://doi.org/10.1007/s11082-023-05983-3.
10. S. K. Saini and S. K. Awasthi, Sensing and Detection Capabilities of One-Dimensional Defective Photonic Crystal Suitable for Malaria Infection Diagnosis from Preliminary to Advanced Stage: Theoretical Study, Crystals, **13**, 128 (2023), https://doi.org/10.3390/cryst13010128.
11. H. S. Ashour, K. M. Abohassan, M. M. Abadla, and A. M. Almaghari, Design and analysis of efficient biosensors based on 1D ternary photonic crystals for malaria detection, *Mod. Phys. Lett*., B **39**, 205057 (2025). https://doi.org/10.1142/S0217984925502057.
12. S. Sen, M. Abdullah-Al-Shafi, M. Mubassera, and H. Hawlader, A high-sensitivity photonic crystal fibre biosensor for malaria detection Sens. Bio-Sens. Res. **51**, 100963 (2026). https://doi.org/10.1016/j.sbsr.2026.100963.
13. M. Medhat, C. Malek, M. Tlija, M. R. Abukhadra, S. Bellucci, H. A. Elsayed, and A. Mehaney, One-Dimensional Photonic Crystals Comprising Two Different Types of Metamaterials for the Simple Detection of Fat Concentrations in Milk Samples, *Nanomaterials,* **14**(21), 1734 (2024) https://doi.org/10.3390/nano14211734.
14. H.-C. Chou, R. G. Bikbaev, I. V. Timofeev, M.-J. Lee, and W. Lee, Simulation of an Asymmetric Photonic Structure Integrating Tamm Plasmon Polariton Modes and a Cavity Mode for Potential Urinary Glucose Sensing via Refractive Index Shifts, *Biosensors,* **15**(10), 644 (2025). https://doi.org/10.3390/bios15100644.
15. M. A. Butt, Emerging Trends in Thermo-Optic and Electro-Optic Materials for Tunable Photonic Devices, *Materials,* **12**, 2782 (2025). https://doi.org/10.3390/ma18122782
16. G. Rego, Temperature Dependence of the Thermo-Optic Coefficient of SiO_2 Glass, *Sensors,* **23**(13), 6023 (2023). https://doi.org/10.3390/s23136023.
17. W. Bai et al., Bioresorbable Multilayer Photonic Cavities as Temporary Implants for Tether-Free Measurements of Regional Tissue Temperatures, *BME Frontiers*, **2021**, 8653218, (2021). https://doi.org/ 10.34133/2021/8653218.
18. D. Sampath, and V. Narasimhan, One-Dimensional Defect Layer Photonic Crystal Sensor for Purity Assessment of Organic Solvents, *ACS Omega*, **9**(8), 9625 (2024). https://doi.org/10.1021/acsomega.3c09589.
19. A. H. Aly, S. K. Awasthi, D. Mohamed, Z. S. Matar, M. Al-Dossari, and A. F. Amin, Study on a one-dimensional defective photonic crystal suitable for organic compound sensing applications, *RSC Adv*. **11**, 32973 (2021). https://doi.org/10.1039/D1RA06513K.
20. J. Barvestani, Topological interface state-based photonic crystal sensor with porous cap layer for high-performance biosensing, *Sci. Rep*. **15**, 43675 (2025). https://doi.org/10.1038/s41598-025-27526-4.

مستشعر بصري متعدد الطبقات مع تجويف دموي للكشف عن الملاريا باستخدام تقنية التوزيع المنعكس المتعدد (DBR): تتبع الرنين، الحساسية الحرارية، وتحليل توزيع الحقل الكهربائي

صادق عبدالله محمد الجبهة[1] وفاهم يحيى احمد بجاش[1]
قسم الفيزياء، كلية التربية والعلوم، جامعة البيضاء، اليمن

الخلاصة

يهدف هذا العمل إلى تقديم دراسة عددية لمستشعر بصري حيوي متعدد الطبقات يعتمد على عواكس براج الموزعة (DBRs) ، مع وجود تجويف مملوء بالدم. تم استخدام طريقة مصفوفة الانتقال (TMM) ومحاكاتها باستخدام برنامج MATLAB، حيث تم تحليل سلوك الرنين في نطاق الأطوال الموجية من (780-810) نانومتر مع دراسة تأثير تغير درجة الحرارة من 15إلى 40 درجة مئوية، بالتزامن مع تغيير سماكة طبقة السيليكون من 20إلى 200 نانومتر.أظهرت النتائج حدوث انزياح أزرق في الأطوال الموجية الرنينية لنمط العيب نتيجة تغير درجة الحرارة، مما أدى إلى ظهور حساسية حرارية سالبة يعتمد مقدارها بصورة غير خطية على سماكة طبقة السيليكون كما أوضحت توزيعات شدة المجال الكهربائي عند الرنين أن السماكات المتوسطة لطبقة السيليكون تؤدي إلى تموضع أقوى للنمط داخل التجويف، الأمر الذي يعزز التفاعل بين الضوء والمادة ويزيد من مقدار الانزياح الطيفي الناتج عن تغير درجة الحرارة. في المقابل، تؤدي طبقات السيليكون ذات السماكات الأكبر إلى إعادة توزيع الطاقة الضوئية داخل مرايا براج، مما يسهم في تقليل الانجراف الحراري من خلال حدوث تعويض جزئي. تشير هذه النتائج إلى أن الضبط الهندسي لمعاملات العواكس الموزعة من نوع براج يمكن أن يحسن بشكل ملحوظ من حصر الرنين واستجابة درجة الحرارة، الأمر الذي يدعم استخدام البنية المقترحة كمنصة استشعار حيوي بصري خالية من الوسم (Label-Free) للتشخيص الدموي المرتبط بمرض الملاريا.

الكلمات المفتاحيه: براغ، مستشعر حيوي، بصري حراري، الملاريا،عاكسات براغ الموزعة.